

Thermal conductivity of pure and Mg-doped CuGeO_3 in the incommensurate phase

J. Takeya, I. Tsukada and Yoichi Ando

Central Research Institute of Electric Power Industry, Komae, Tokyo 201-8511, Japan

T. Masuda and K. Uchinokura

Department of Advanced Materials Science, The University of Tokyo, Bunkyo-ku, Tokyo 113-8656, Japan

I. Tanaka* and R. S. Feigelson

Center for Material Research, Stanford University, Stanford, CA 94305

A. Kapitulnik

E. L. Ginzton Laboratory, Stanford University, Stanford, CA 94305

(Received November 17, 2018)

The thermal conductivity κ of $\text{Cu}_{1-x}\text{Mg}_x\text{GeO}_3$ is measured in magnetic fields up to 16 T. At the transition field H_c to the high-field incommensurate (I) phase, κ abruptly decreases. While κ of the pure CuGeO_3 is enhanced with the application of higher magnetic fields, an anomalous plateau feature shows up in the $\kappa(H)$ profile in the I phase of the Mg-doped samples which includes antiferromagnetic ordering (I-AF phase). With the help of specific heat data, taken supplementally for the identical samples, the above features are well understood that phonons are strongly scattered by spin solitons and that κ in the I phase is governed by their spatial distribution. In particular, the plateau feature in the doped samples suggests “freezing” of the solitons, in which antiferromagnetism must be playing an essential role because this feature is absent at temperatures above T_N .

PACS numbers: 66.70.+f, 75.30.Kz, 75.50.Ee

I. INTRODUCTION

Recently, a new class of commensurate-incommensurate (C-I) transition, magnetic-field induced C-I transition, which had been theoretically predicted,¹ was experimentally established in an one-dimensional antiferromagnetic (AF) Heisenberg spin system coupled to lattice degrees of freedom, the spin-Peierls (SP) system; the magnetic transition is observed in magnetization measurements^{2,3} and the incommensurate lattice modulation is visibly shown in x-ray diffraction experiments.^{4,5} The SP system shows a transition at T_{SP} from the uniform (U) spin-1/2 quantum liquid phase to the dimerized (D) phase, where spin-singlet ground state is formed at the expense of the lattice deformation energy.⁶ With the application of magnetic field, a new magnetic phase appears above a threshold field H_c because the nonmagnetic spin-singlet state becomes energetically unfavorable in high magnetic fields. The magnetic moment is partly recovered in the chain, and “spin solitons” are formed in this magnetic phase. The “spin soliton” contains both lattice deformation and moment (carrying spin 1/2), whose spatial distribution is governed by the sine-Gordon equation. Usually, the periodicity of the solitons are determined simply by the applied magnetic field, and as a result, the spin and lattice modulation becomes incommensurate. Therefore, this high-field phase is called incommensurate (I) phase. After the existence of the incommensurate modulation is established, the subsequent interest on this I phase is how the spin and lattice mod-

ulation evolves under higher magnetic fields (well above H_c), where the soliton distance becomes comparable to the soliton width.⁷⁻⁹

The discovery of the inorganic SP compound CuGeO_3 (Ref. 10) opened the way to impurity substitution and it turned out that just a small amount of the impurity modifies the phase diagram to a more complicated one;^{11,12} with decreasing temperature, after the appearance of D phase at T_{SP} , the system shows another transition to a peculiar ordered phase, where antiferromagnetic (AF) long-range order and the SP order coexist [dimerized AF (D-AF) phase].¹³ The staggered moment and the lattice deformation are spatially modulated in D-AF phase; the amplitude is larger near the impurity sites and smaller in between them.^{14,15} In contrast to such well-established pictures of the ordered phase in low fields (D and D-AF phase), the spin distribution in high-field phases of the impurity-doped systems is still under question. Also, the phase boundaries for the high-field phases are not yet investigated for the system with its Cu site substituted by impurities (Cu-O chains are directly disordered), although there exist several reports on these phase boundaries for the system whose Ge site is substituted. Recently, we reported that κ of $\text{Cu}_{1-x}\text{Mg}_x\text{GeO}_3$ is sensitive to the Mg-doping (disorder),^{16,17} and demonstrated that such transport measurement is useful in examining the disorder effects. In this work, we have measured the thermal conductivity of $\text{Cu}_{1-x}\text{Mg}_x\text{GeO}_3$ single crystals with the application of magnetic field up to 16 T. The specific heat is also measured supplementally for the iden-

tical samples. First, κ of the pure CuGeO_3 is measured in order to identify the dominant scattering mechanism in the I phase. It turned out that the dominant heat carriers (phonons) are strongly scattered with the appearance of the spin solitons in the I phase, indicating that κ is a good probe of the soliton distribution. Our main result is an anomalous plateau feature found in the $\kappa(H)$ profile in the antiferromagnetically ordered I (I-AF) phase of the Mg-doped samples, suggesting that the spin solitons are frozen in the I-AF phase.

II. EXPERIMENTAL

The single crystals of $\text{Cu}_{1-x}\text{Mg}_x\text{GeO}_3$ were grown with a floating-zone method. We have prepared both pure CuGeO_3 (the SP transition temperature $T_{\text{SP}}=14.5$ K) and two Mg-doped samples $x = 0.016$ and $x = 0.0216$ with T_{SP} 's of 11.5 K and 9 K, respectively. (The T_{SP} 's are determined by dc magnetization measurements). The Mg concentration is carefully determined by inductively coupled plasma-atomic emission spectroscopy (ICP-AES).¹⁸ The Mg-doped samples shows the Néel transition at $T_N = 2.5$ K and 3 K, respectively.^{13,18} Masuda *et al.* carefully examined x dependence of the T_N for the same series of crystals and found that T_N jumps at the impurity-driven transition from the D-AF phase to the uniform AF phase without dimerization.^{13,18} Note that the D-AF phase shows up below T_N in the sample used for our present study because the Mg concentration of the both samples is smaller than the critical concentration x_c ($= 0.023 \sim 0.027$).^{13,18}

The thermal conductivity is measured using a “one heater, two thermometers” method. The direction of the heat current and the magnetic field is parallel to the c -axis, i.e., the chain direction. The detailed experimental technique is described elsewhere.^{16,19} Since the total thermal conductivity is expressed as $\kappa = \sum C_i D_i$, where C_i and D_i are specific heat and diffusivity of each heat carrier denoted by i (the diffusivity D_i is proportional to the mean free path of the heat carrier), the specific heat measurement is helpful in the analysis of the κ data. We have measured the specific heat in magnetic fields up to 16 T by the usual relaxation method for the same samples. The addenda consists of a sapphire substrate, a cernox temperature sensor (calibrated in magnetic fields) and 1-k Ω micro heater. The connection from the addenda to the heat sink is made by Sb-Au thin wires to provide a moderate heat-relaxation rate, from which the heat capacity is calculated.

III. RESULTS

A. Pure CuGeO_3

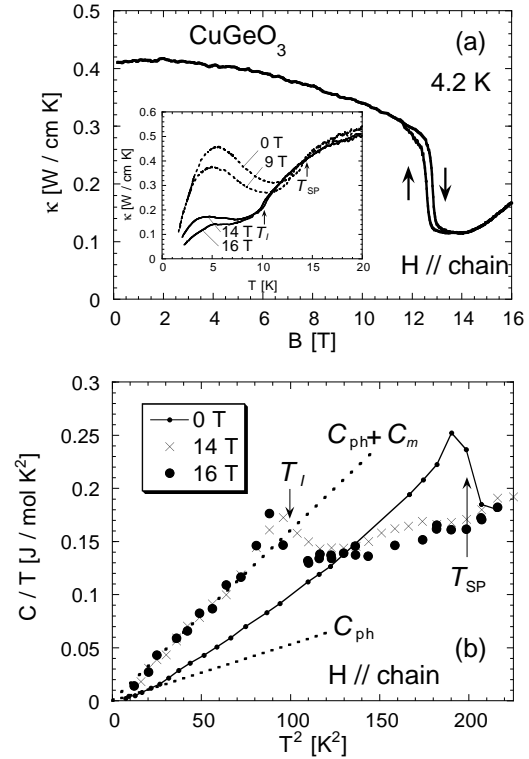


FIG. 1. (a) Magnetic field dependence of the thermal conductivity of CuGeO_3 single crystal at 4.2 K. The magnetic field is applied in the c -axis direction. First order transition from the spin-Peierls to the incommensurate phase takes place at H_c . Inset: temperature dependence of the thermal conductivity of CuGeO_3 in magnetic fields. T_{SP} and T_I are the transition temperatures below which spin-Peierls phase and incommensurate phase appear, respectively. (b) C/T in magnetic fields is plotted as a function of T^2 . The dotted line for the 0-T curve indicates the T^3 dependence of the phonon contribution C_{ph} . The other dotted line for the C/T curves in the I phase shows that the additional magnetic contribution C_m also depends on temperature as T^3 .

The inset of Fig. 1(a) shows the temperature dependence of κ in fields up to 16 T. The transition temperatures from the U phase to the D phase (below 9 T) and to the I phase (above 14 T) are indicated as T_{SP} and T_I , respectively. While both phonons and spin excitations carry a large amount of heat in the U phase,^{16,19} phonons become the dominant heat carrier at temperatures well below T_{SP} in the D phase because of the spin gap. These phonons are mostly scattered by defects at the lowest temperatures, where spin excitations are almost absent, and field dependence is small there; the 0-T and 9-T curves merge below ~ 3 K. When thermally excited spin excitations increase with temperature and the scattering rate of the phonons are enhanced, via spin-phonon coupling, κ starts to decrease with temperature, producing a pronounced peak around ~ 5 K.¹⁹ Since this peak in

κ is a manifestation of the spin gap, the peak height is rapidly suppressed with magnetic fields.¹⁶

The field dependence of κ at 4.2 K is presented in the main panel of Fig. 1(a) to see the suppression of the peak under magnetic fields. A sudden drop in κ , accompanied by hysteresis, shows up at the first order transition from the D phase to the I phase ($H_c \sim 12.5$ T). When the magnetic field increases above H_c , κ starts to increase at ~ 14 T. The specific heat C is measured for the same sample in order to elucidate the origin of the field dependence of κ ($\kappa_i = C_i D_i$). The 14-T and 16-T data are plotted together with zero-field data in Fig. 1(b). In contrast to κ , C in the I phase is *larger* than that in the D phase below $T_I \sim 10$ K, indicating that the jump in κ at H_c is caused by a sudden change in *diffusivity*. It is also to be noted that the values of C at 14 T and at 16 T do not significantly differ below T_I , while κ shows an apparent increase above 14 T, suggesting the enhancement in the diffusivity D_i with the field application above ~ 14 T.

B. Mg-doped CuGeO_3

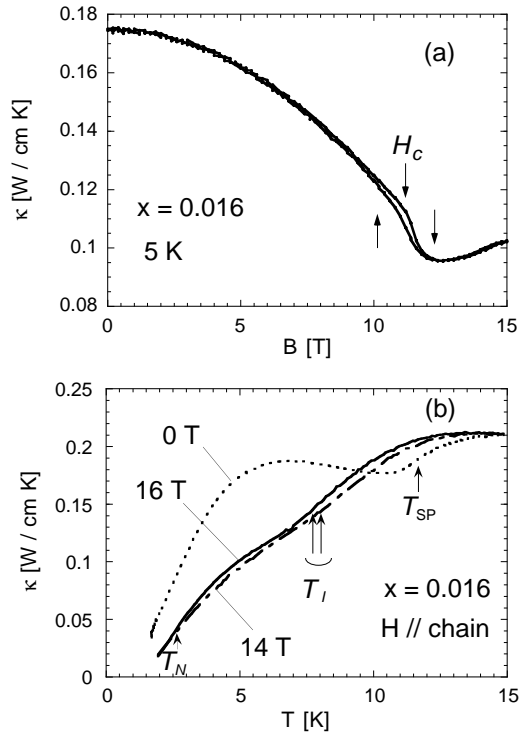


FIG. 2. (a) Magnetic field (along the CuO chain) dependence of the thermal conductivity of $\text{Cu}_{1-x}\text{Mg}_x\text{GeO}_3$ with $x = 0.016$ at 5 K. (b) Temperature dependence of κ in magnetic fields up to 16 T for the $x = 0.016$ sample. T_N indicates the Néel transition in the I phase.

Figure 2(a) shows the $\kappa(H)$ profile of the $x = 0.016$ sample at 5 K, which is above the zero-field T_N (~ 2 K), determined from dc magnetization. Similarly to the pure sample [Fig. 1(a)], κ is rapidly suppressed with magnetic

field when the field approaches $H_c \sim 11.5$ T, and then increases in the field range above H_c . Hysteresis is observed in the vicinity of H_c also for this sample, although the transition becomes broader.

The temperature dependence of κ is shown in Fig. 2(b). The transition temperatures T_{SP} and T_I are indicated with arrows (together with T_N). Note that the 14-T and 16-T curves merge below T_N , suggesting field independent $\kappa(H)$ above H_c in this temperature range. Since this feature is expected to be more pronounced for a sample with higher T_N , we measured the field dependence of the $x = 0.0216$ sample. Figure 3(a) presents $\kappa(H)$ profiles at the temperatures of 2.5 K and 5 K. An apparent plateau is observed above $H_c \sim 11.5$ T in the 2.5-K curve, while the 5-K curve shows a slight upturn above H_c , similarly to the field profile in the I phase of the pure sample. Figure 3(b) shows the temperature dependence of κ in three different fields above H_c and that without magnetic field. One can see that the 12-, 14- and 16-T curves merge below ~ 4 K, which is close to zero-field T_N (~ 3 K).

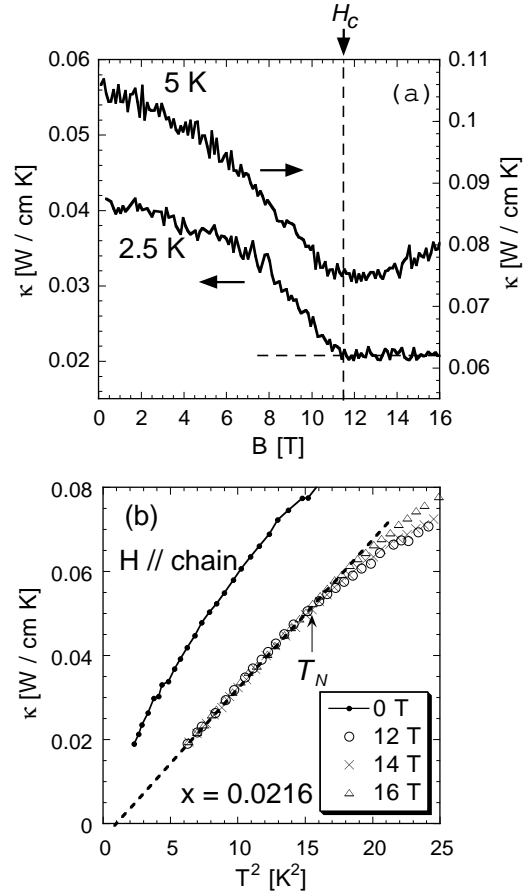


FIG. 3. (a) Magnetic field dependence of the thermal conductivity of $\text{Cu}_{1-x}\text{Mg}_x\text{GeO}_3$ with $x = 0.0216$ at 2.5 K. $\kappa(H)$ becomes independent of magnetic fields in the I phase (above H_c). (b) κ in magnetic fields up to 16 T is plotted against T^2 for the $x = 0.0216$ sample. Below T_N , all the curves for the I phase merges to a single line. The dotted line shows that κ is mostly proportional to T^2 below T_N .

Figure 4 shows the temperature dependence of the specific heat of the same $x = 0.0216$ sample. The 16-T curve shows a λ -shaped anomaly, indicating that T_N under this magnetic field is around 4 K, just below which the plateau feature appears in the $\kappa(H)$ profile. Note that T_N at 16 T is apparently higher than the zero-field T_N , because the spin fluctuation is reduced by field application.^{20,21} It is also notable that a broad anomaly is observed above T_N up to ~ 8.5 K, suggesting the existence of another phase at higher temperatures.

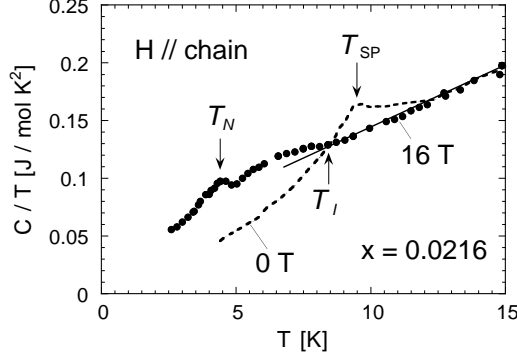


FIG. 4. Specific heat of the $x = 0.0216$ sample. The I phase and the I-AF phase appear below T_I and T_N , respectively. The solid line is a guide to determine T_I .

IV. DISCUSSION

A. Soliton scattering in I phase

First, let us consider the $\kappa(H)$ profile at 4.2 K shown in Fig. 1(a). The dominant heat carriers are phonons in the pure CuGeO_3 well below T_{SP} , where the spin excitations are hardly excited because of the spin gap. Therefore, $\kappa(H)$ shown in Fig. 1(a) mostly reflects the field dependence of κ_{ph} at least below H_c . When the population of the spin excitations gradually increases with field, the scattering by the spin excitations increases and, as the result, κ_{ph} slowly decreases.

While the major part of the specific heat is due to phonons in the D phase, the additional component, i.e., magnetic specific heat C_m , appears in the I phase, as shown in Fig. 1(b). This result reproduces the report by Lorenz *et al.*,²² and is consistent with the theory claiming that C_m is due to magnetoelastic excitations called phasons.²³ Since both C_m and C_{ph} depends on temperature as $\propto T^3$, the total C is $\propto T^3$. The thermal conductivity is given by $\kappa = \sum C_i D_i$ ($i = \text{ph}, m$), where

the additional magnetic specific heat C_m reaches twice as large as the phonon contribution C_{ph} [see Fig. 1(b)]. Nevertheless, κ suddenly *decreases* at the transition from the D phase to the I phase, meaning that the decrease in κ_{ph} is dominant at the transition, though the newly appearing phasons could also carry some heat. Since little change in C_{ph} is expected at H_c , it must be D_{ph} that is responsible for the abrupt change in $\kappa(H)$, indicating the sudden appearance of new scatterers of phonons in the I phase. It is most likely that phonons are strongly scattered by domain walls accompanied with the spin solitons, which would be equivalent to the scattering by the phasons. Note that the ultra-sonic results, in which sudden change in elastic constants was shown at H_c , are understood in terms of the phonon-soliton interaction.²⁴

The $\kappa(H)$ profile above H_c also is not simply explained by C in the I phase; κ increases above ~ 14 T, while the difference in C_m at 14 T and that at 16 T is negligible within the accuracy of our measurement ($\sim 10\%$ of C_m),²⁵ as shown in Fig. 1(b). Since the enhancement in κ from 14 T to 16 T is more than four times larger than this maximum error, the diffusivity should be responsible for the magnetic-field dependence of κ also in the field range above H_c .

Assuming that $D_{ph}(H)$ is governed by the scattering by the domain walls in the I phase, as is discussed above, $D_{ph}(H)$ should be modified when the soliton distribution changes with field. In a sufficiently high magnetic field where the soliton distance d becomes comparable to the soliton width ξ , the adjacent solitons would overlap with each other and the lattice and spin modulation might become sinusoidal wave, as is suggested by a recent NMR measurement^{7,9} and a magnetostriction result.⁸ It is expected that the cross section of the domain-wall scattering is smaller for the sinusoidal-wave modulation than for the independent solitons, because the amplitude of the lattice modulation is smaller for the sinusoidal-wave distribution. Such field dependence of the soliton distribution well explains the enhancement in $D_{ph}(H)$ with field above H_c , and is consistent with the $\kappa(H)$ profile in the I phase. The ratio of d/ξ is ~ 2.3 at ~ 14 T (Ref. 7) where the overlapping becomes evident in $\kappa(H)$.

B. Incommensurate phases in the Mg-doped samples

Since κ and C data demonstrate anomalies at the transition temperatures and at the critical field, we can discuss the phase boundary for the high-field phases of the Mg-doped CuGeO_3 . So far, contradictory results are reported on the high-field incommensurate phases for CuGeO_3 crystals whose Ge site is substituted by Si. Two transitions are observed in the specific heat measurement; one is from the U phase to the incommensurate phase without AF ordering (I phase) and the other is a Néel transition from this I phase to the I-AF phase.²¹ On the

other hand, the result of a ultrasound-velocity measurement suggests a direct transition from the U phase to the I-AF phase.²⁶

Let us discuss this problem on the basis of our κ and C data for the Mg-doped samples, where Cu-O chain is directly modulated. The Néel transition to the I-AF phase is apparent also for the Mg-doped samples; the specific heat shows a clear λ -shaped peak (Fig. 4), and the field dependence of κ disappears as shown in Fig. 2(b) and Fig. 3(b). In addition to the features at the Néel ordering, an enhancement is observed below $T_I \sim 9$ K in κ for the $x = 0.016$ sample [Fig. 2(b)]. The specific heat data for the $x = 0.0216$ sample in 16 T also shows an enhancement below $T_I \sim 8.5$ K (Fig. 4). The results indicate the existence of the I phase without AF order for the Mg-doped samples.²⁷ However, the anomaly in the C data is not so obvious at T_I as at T_N . This is probably because of the existence of short-range ordered (SRO) state in the SP transition in the impurity-doped CuGeO_3 . Noting that long-range SP order is not established down to ~ 6.5 K at 0 T for the $x = 0.0216$ sample (Ref. 18,28), and assuming the SRO state also in magnetic fields above H_c , the “transition temperature T_I ” will not be well-defined.

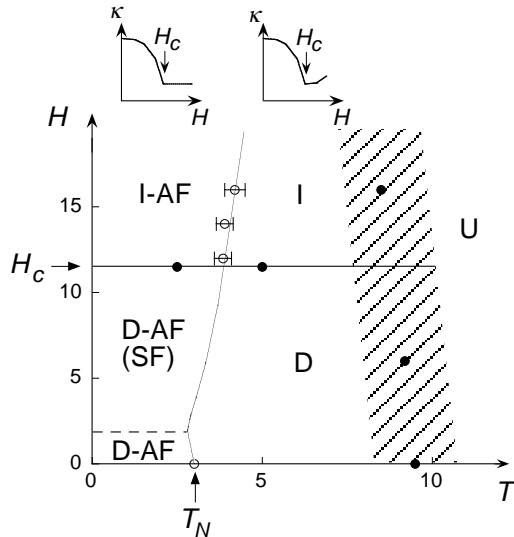


FIG. 5. The schematic H - T phase diagram of the $x = 0.0216$ sample, based on the results of the κ and C measurements. Open and closed circles indicate the transition temperatures determined from the κ and C data. The hatched area indicates the short-range ordered regime.

The field induced transition from D to I and from D-AF to I-AF phases at H_c is also evident in the $\kappa(H)$ profile; κ for the $x = 0.016$ sample and the two curves for the $x = 0.0216$ sample (at 2.5 K and 5 K) rapidly decrease (with hysteresis when $x = 0.016$) with the application of magnetic fields below $H_c \sim 11.5$ T, while the decrease abruptly disappears above H_c [Fig. 2(a) and Fig. 3(a)], similarly to the D-I transition observed for the pure CuGeO_3 . Note that the transition at 5 K (above $T_N \sim 4$ K) and that at 2.5 K (below T_N) take

place at almost the same field around $H_c \sim 11.5$ T, i.e., the value of H_c is irrelevant to whether the temperature is above or below T_N . The above results suggest that both transitions, from D to I and from D-AF to I-AF, are “commensurate-incommensurate” transition, which is characterized by the appearance of the spin solitons. The suggested phase diagram is presented in Fig. 5, following the discussion in this subsection.

C. Freezing of the solitons in I-AF phase

The most striking observation in the $\kappa(H)$ profile for the Mg-doped samples is the plateau feature which appears in the I-AF phase [see Fig. 3(a)]. Since the plateau suddenly appears above H_c , it should be related to the specific scattering mechanism in the incommensurate phase, i.e., the scattering by the domain-walls. Therefore, the field independence in the I-AF phase suggests that the soliton population and their distribution are *not* affected by the magnitude of the applied magnetic field, indicating that the solitons are frozen. Since the plateau in $\kappa(H)$ is present only below T_N [see Fig. 3(b)], it is the specific feature of the I-AF phase, and the AF order must be essential for the soliton freezing.

In the I-AF phase, it is suggested that solitons are preferably distributed around the impurity sites and that staggered moments are distributed also in between these solitons.²⁹ Since the spin-flop transition takes place at ~ 1 T,^{30,31} the staggered moments are directed almost perpendicular to H in the I-AF phase. When the magnetic field increases, there are two ways to gain the magnetic energy ΔMH , where ΔM is the additional magnetization: one is to append other solitons in between the impurity sites, though this position is not so favored compared to the impurity sites, and the other is to cant the staggered moments to the direction of H . The second process can give an origin of the soliton “freezing” induced by the antiferromagnetism, because the soliton distribution is preserved under further magnetic field. Although the above scenario gives a plausible explanation, independent measurements by neutron scattering and/or NMR are required to elucidate this microscopic mechanism of the antiferromagnetism-induced soliton freezing.

The dotted line in Fig. 3(b) indicates that κ is proportional to T^2 when the sample is cooled below T_N . Since the specific heat have the temperature dependence of $\propto T^3$, the diffusivity should behave as $\propto 1/T$, the typical temperature dependence of κ_{ph} when phonons are scattered by dislocations of solids, like defects. The observation shows that the domain walls of the spin solitons behave as rigid dislocations, which would be consistent with the above picture of the frozen solitons in the I-AF phase.

V. SUMMARY

The results of the thermal conductivity measurement on both pure and Mg-doped CuGeO_3 , accompanied with the specific heat measurement for the same crystals, help to further understand the high-field incommensurate phase of the SP system, the spin-soliton phase. First, it turned out that the phonon transport in the I phase is governed by the domain-wall scattering due to the significant phonon-soliton interaction, and is strongly influenced by spatial distribution of the solitons. Since the kink features in H and T dependence caused by the appearance (change in the distribution) of the solitons tell us the transition into (in) the I phase, the $H - T$ phase diagram of the Mg-doped CuGeO_3 (where the CuO chain is directly disturbed), is established. Based on our result of $\kappa(H)$ above H_c , it is suggested that the spin solitons are frozen in the I-AF phase with the help of the AF ordering, providing a clue for the full understanding of the spin distribution in this unusual coexistence phase.

VI. ACKNOWLEDGMENT

We greatly thank M. Saito for fruitful discussions.

* Present address: Institute of Inorganic Synthesis, Faculty of Engineering, Yamanashi University, Kofu, Yamanashi 400, Japan.

- ¹ A. M. Kosevich and V. I. Khokhlov, *Solid. State. Commun.* **11**, 461 (1972); M. C. Cross and D. S. Fisher, *Phys. Rev. B* **19**, 402 (1979); M. C. Cross, *Phys. Rev. B* **20**, 4606 (1979); T. Nakano and H. Fukuyama, *J. Phys. Soc. Jpn.* **49**, 1679 (1980); *ibid.*, **50**, 2489 (1981); B. Horovitz, *Phys. Rev. Lett.* **49**, 742 (1981).
- ² See e.g., J. W. Bray, L. V. Interrante, I. S. Jacobs, D. Bloch, D. E. Moncton, G. Shirane, and J. C. Bonner, *Phys. Rev. B* **20**, 2067 (1979); D. Bloch, J. Voiron, J. C. Bonner, J. W. Bray, I. S. Jacobs, and L. V. Interrante, *Phys. Rev. Lett.* **44**, 295 (1980).
- ³ M. Hase, I. Terasaki, K. Uchinokura, M. Tokunaga, N. Miura, and H. Obara, *Phys. Rev. B* **48**, 9616 (1993).
- ⁴ V. Kiryukhin, B. Keimer, and D. E. Moncton, *Phys. Rev. Lett.* **74**, 1669 (1995).
- ⁵ V. Kiryukhin, B. Keimer, J. P. Hill, and A. Vigliante, *Phys. Rev. Lett.* **76**, 4608 (1996).
- ⁶ See e.g. J. W. Bray, L. V. Interrante, I. C. Jacobs, and J. C. Bonner, in *Extended Linear Chain Compounds*, ed. J. C. Miller (Plenum Press, New York, 1983), p. 353.
- ⁷ M. Horvatić, Y. Fagot-Revurat, C. Berthier, G. Dhalenne, and A. Revcolevschi, *Phys. Rev. Lett.* **83**, 420 (1999).
- ⁸ T. Lorenz, B. Büchner, P. H. M. van Loosdrecht,

- F. Schöfneld, G. Chouteau, A. Revcolevschi, and G. Dhalenne, *Phys. Rev. Lett.* **81**, 148 (1998).
- ⁹ G. S. Uhrig, F. Schöfneld, J.-P. Boucher, and M. Horvatić, *Phys. Rev. B* **60**, 9468 (1999).
- ¹⁰ M. Hase, I. Terasaki, and K. Uchinokura, *Phys. Rev. Lett.* **70**, 3561 (1993).
- ¹¹ M. Hase, I. Terasaki, Y. Sasago, K. Uchinokura, and H. Obara, *Phys. Rev. Lett.* **71**, 4059 (1993).
- ¹² K. Manabe, H. Ishimoto, N. Koide, Y. Sasago, and K. Uchinokura, *Phys. Rev. B* **58**, R575 (1998).
- ¹³ T. Masuda, A. Fujioka, Y. Uchiyama, I. Tsukada, and K. Uchinokura, *Phys. Rev. Lett.* **80**, 4566 (1998).
- ¹⁴ H. Fukuyama, T. Tanimoto, and M. Saito, *J. Phys. Soc. Jpn.* **65**, 1182 (1996).
- ¹⁵ K. M. Kojima, Y. Fudamoto, M. Larkin, G. M. Luke, J. Merrin, B. Nachumi, Y. J. Uemura, M. Hase, Y. Sasago, K. Uchinokura, Y. Ajiro, A. Revcolevschi, and J. P. Renard, *Phys. Rev. Lett.* **79**, 503 (1997).
- ¹⁶ J. Takeya, Y. Ando, T. Masuda, I. Tsukada, and K. Uchinokura, *Phys. Rev. B*, in press, cond-mat/9905228.
- ¹⁷ J. Takeya, Y. Ando, T. Masuda, I. Tsukada, and K. Uchinokura, preprint, cond-mat/0004367.
- ¹⁸ T. Masuda, I. Tsukada, K. Uchinokura, Y. J. Wang, V. Kiryukhin, and R. J. Birgeneau *Phys. Rev. B* **61**, 4103 (2000).
- ¹⁹ Y. Ando, J. Takeya, D. L. Sisson, S. G. Döttinger, I. Tanaka, R. S. Feigelson, and A. Kapitulnik, *Phys. Rev. B* **58**, R3651 (1998).
- ²⁰ T. Masuda *et al.*, in preparation.
- ²¹ M. Hiroi, T. Hamamoto, M. Sera, H. Nojiri, N. Kobayashi, M. Motokawa, O. Fujita, A. Ogiwara, and J. Akimitsu, *Phys. Rev. B* **55**, R6125 (1997).
- ²² T. Lorenz, U. Ammerahl, R. Ziemes, B. Büchner, A. Revcolevschi, and G. Dhalenne, *Phys. Rev. B* **54**, R15610 (1996).
- ²³ S. M. Bhattacharjee, T. Nattermann, and C. Ronnewinkel, *Phys. Rev. B* **58**, 2658 (1998).
- ²⁴ M. Saint-Paul, G. Reményi, N. Hegman, P. Monceau, G. Dhalenne, and A. Revcolevschi, *Phys. Rev. B* **55**, R6121 (1997).
- ²⁵ Recently, precise $C(H)$ profile was reported up to 22 T [G. Reményi, N. Hegman, J. C. Lasjaunias, S. Sahling, G. Dhalenne, and A. Revcolevschi, *Czek. J. Phys.* **46 S4**, 1959 (1996)]. According to their results, the difference in C_m at 14 and 16 T is sample dependent and is at most $\sim 6\%$.
- ²⁶ M. Poirier, R. Beaudry, M. Castonguay, M. L. Plumer, G. Quirion, F. S. Razavi, A. Revcolevschi, and G. Dhalenne, *Phys. Rev. B* **52**, R6971 (1995).
- ²⁷ The same conclusion is obtained independently by Masuda *et al* [Ref. 20] by specific heat measurement using the same series of crystals.
- ²⁸ Y. J. Wang, V. Kiryukhin, R. J. Birgeneau, T. Masuda, I. Tsukada, and K. Uchinokura, *Phys. Rev. Lett.* **83**, 1676 (1999).
- ²⁹ M. Saito, *J. Phys. Soc. Jpn.* **67**, 2477 (1998).
- ³⁰ M. Hase, N. Koide, K. Manabe, Y. Sasago, K. Uchinokura, and A. Sawa, *Physica B* **215**, 164 (1995).
- ³¹ H. Nojiri, T. Hamamoto, Z. J. Wang, S. Mitsudo, M. Motokawa, S. Kimura, H. Ohta, A. Ogiwara, O. Fujita, and J. Akimitsu, *J. Phys. C* **9**, 1331 (1997).